

Rotational Dynamics of Adamantanecarboxylic Acid in Complex with β -cyclodextrin

ZDENĚK TOŠNER^{1,2,*}, SAHAR NIKKHOU ASKI¹ and JOZEF KOWALEWSKI¹

¹Department of Physical, Inorganic and Structural Chemistry, Arrhenius Laboratory, Stockholm University, SE-106 91 Stockholm, Sweden; ²Department of Low Temperature Physics, Faculty of Mathematics and Physics, Charles University, V Holešovičkách 2, CZ-180 00 Prague 8, Czech Republic

(Received: 10 May 2005; in final form: 12 September 2005)

Key words: 1-adamantanecarboxylic acid, β -cyclodextrin, host–guest complexes, nuclear magnetic resonance, translational diffusion, rotational dynamics

Abstract

The reorientation of 1-adamantanecarboxylic acid (AdCA) within the β -cyclodextrin (β -CD) cavity is investigated by means of multiple-field ¹³C NMR relaxation. The dissociation constant describing the complexation equilibrium is determined using translational diffusion measurements for the guest during a titration by the host in D₂O/DMSO solvent mixture. The changes in apparent diffusion properties of AdCA during the titration are at 25 °C well described assuming the formation of a 1:1 complex, whereas at 0 °C the data indicate the presence of a 2:1 (guest:host) complex. The ¹³C NMR relaxation parameters for the AdCA molecule bound inside the β -CD cavity are extracted. Despite the high association constant, indicating a strong interaction between the two molecules, the guest molecule is quite mobile. The reorientation of the bound AdCA at 25 °C can be described by either the Lipari–Szabo or the axially symmetric rotational diffusion model. The motion is extremely anisotropic: the adamantyl group rotates fast around the β -CD symmetry axis, inside its cylindrical cavity. At lower temperature, the relaxation properties are no longer possible to explain using these models. Instead, the data are analyzed using extended, three-step spectral density of Clore et al. [*J. Am. Chem. Soc.* **112**, 4989 (1990)].

Introduction

Over the past years, there has been considerable interest in studying the nanoscale molecular containers (hosts) that are able to incorporate small neutral guest species [1]. These nanocavities are used for selective binding, separation and sensing of smaller molecules and ions, molecular transport and delivery, stabilization of reactive intermediates, and catalysis through encapsulation. They also can provide useful models of ligand binding in larger biological molecules (e.g., hydrophobic pockets of enzymes) [1].

One class of such molecular hosts are cyclodextrins [2], which usually contain 6–8 glucose units connected in a macrocyclic ring and take shape of a truncated cone with a hydrophobic cavity. The primary hydroxyl groups, OH-6, are oriented towards the narrower opening of the molecule and the secondary hydroxyl groups, OH-2 and OH-3, are oriented to the other side. The principal factors involved in cyclodextrin inclusion complexes are believed to be van der Waals and hydrophobic interactions, although hydrogen bonding

and steric effects also have certain roles to play [3]. Overall, the primary consideration for both the complex stability, the guest position and the dynamics appears to be the shape and size of the guest molecule. The guest must satisfy the size criterion of fitting at least partially into the cavity. The most probable mode of binding involves the insertion of a less polar part of the guest molecule into the cavity, while a more polar, and often charged group of the guest is exposed to the bulk solvent just outside of the wider opening. The inclusion complexation by cyclodextrins in an aqueous solution also results in a substantial rearrangement and removal of water molecules originally solvating both the host and the guest [4]. This process includes the release of high-enthalpy water molecules from the cavity to the bulk water.

The internal cavity of β -cyclodextrin (β -CD), which comprises seven glucose units, can contain a large variety of guest molecules [4]. The association constant of the inclusion complex formed between 1-adamantanecarboxylic acid (AdCA) and β -CD is quite large compared to other complexes and is of similar magnitude to many protein–ligand association constants [5]. The β -CD cavity with a volume of 270 Å³ and an average radius of 6.9 Å apparently has the optimum

* Author for correspondence. E-mail: tošner@karlov.mff.cuni.cz

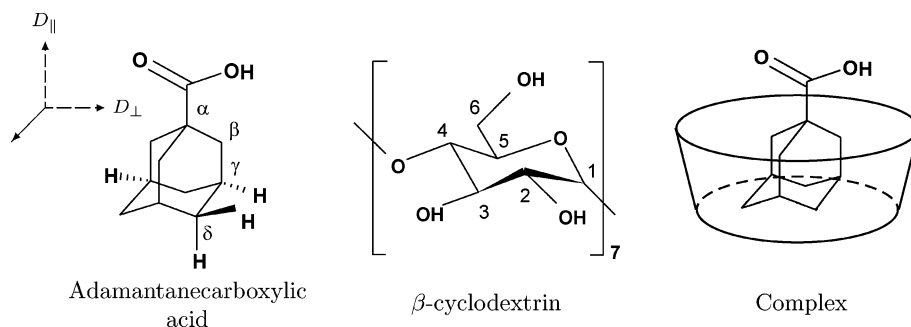


Figure 1. The chemical structures of AdCA and β -CD (with the atom numbering), and the sketch of their complex. The principal axes of the rotational diffusion tensor for AdCA are also indicated.

dimensions for interaction with AdCA [2, 5] – the adamantyl moiety is a spherical group having a radius of about 7 Å and a volume of about 180 Å³ (see Figure 1 for illustration). pH titration studies of adamantane-carboxylate: β -CD complexes show that the neutral carboxylic acid form of the ligand has significantly higher association constant than the anionic form [5]. The binding of the protonated form is found to be more exothermic. An explanation for this phenomenon is that more extensive solvation of the charged carboxylate group by water may prohibit the adamantyl group from fully penetrating the β -CD cavity, whereas deeper penetration may be possible with the neutral carboxylic acid group. This functional group may also form hydrogen bonds with hydroxyl groups on the rim of the β -CD cavity [5].

Nuclear magnetic resonance (NMR) has been widely used in the studies of cyclodextrin complexes [6]. Besides studies of equilibria and structures, NMR can give information on various aspects of molecular dynamics [7]. Studies of nuclear spin relaxation, in particular, allow probing the coupling between the rotational motions of the guest and the host, thus testing the weak interactions in a very direct way [7, 8]. Experiments of this kind were proposed by Behr and Lehn [9]. They studied the molecular motions in inclusion complexes of α -cyclodextrin, using ¹³C and deuterium relaxation. Their results show that, in a general fashion, a molecular complex should be described not only by its thermodynamic stability (or its formation and dissociation constants), but also by its dynamic rigidity/flexibility. This property is defined by the coupling between the molecular motions of the two (or more) entities of which it is composed. This dynamic coupling then reflects, in a way, the strength of the forces involved.

As demonstrated in some studies from our laboratory, the discussions of the dynamic coupling can be put on a firmer ground, if a suitable model for the dynamics is formulated and verified by variable magnetic field relaxations studies outside of the extreme narrowing regime [10, 11]. In this article, we investigate the reorientation of AdCA within the β -CD cavity by means of ¹³C NMR relaxation. We have chosen to work in a D₂O/DMSO solvent mixture, in order to slow down the molecular tumbling and to bring the system out of the

extreme narrowing range, and to increase the solubility of the host. Since earlier studies of the AdCA: β -CD system have been carried out in water [5], a necessary first step in this investigation is to re-evaluate the complexation equilibria.

Methods

NMR provides convenient methods for determining equilibrium constants [12], typically by following changes in chemical shifts during titration. The prerequisites of well-resolved peaks and sufficiently large difference in chemical shift of free and bound form are not always met, especially for aliphatic molecules. On the other hand, molecular association has direct influence on translational diffusion [13]. The self-diffusion coefficient is related to hydrodynamic radius (Stokes–Einstein equation) and thus to the size of the molecule (or the molecular aggregate). The diffusion of a small guest is slowed down significantly when it binds to the large host.

The dissociation constant of a host–guest complex of 1:1 stoichiometry can be expressed in terms of total concentrations of the host and guest ($[H]_0$ and $[G]_0$, respectively) as

$$K_d = \frac{(1-p)([H]_0 - p[G]_0)}{p} \quad (1)$$

where p is the actual population of the complexed guest molecules, $p = [HG]/[G]_0$. In the case of fast exchange (on the chemical shift time scale and comparing to the diffusion interval), the measured diffusion coefficient is the mole-fraction weighted average of diffusion coefficients of free (D_F) and complexed (D_B) forms [14]:

$$D_{\text{obs}} = (1-p)D_F + pD_B \quad (2)$$

The dissociation constant K_d is determined by fitting the changes of D_{obs} measured over a range of host or guest concentrations (combine Equations (1) and (2)). Sometimes it is possible to assume that D_B is equal to the diffusion constant of the host (when the host is much larger than the guest) and only one-parameter fit is necessary.

Another diffusive process, molecular reorientation, can be monitored by means of ¹³C NMR relaxation

[15]. For aliphatic carbon atoms the main relaxation mechanism is a dipole–dipole interaction with directly bonded protons. When the cross-correlation effects can be neglected (by the choice of proper experimental methods) the longitudinal and transverse relaxation times (T_1 and T_2 , respectively), as well as cross-relaxation rate σ are given by Equations (3)–(5). Another relaxation parameter, nuclear Overhauser effect enhancement factor, NOE, is determined by Equation (7):

$$T_1^{-1} = \frac{1}{4} N_{\text{H}} (\text{DCC})^2 [J(\omega_{\text{H}} - \omega_{\text{C}}) + 3J(\omega_{\text{C}}) + 6J(\omega_{\text{H}} + \omega_{\text{C}})] \quad (3)$$

$$T_2^{-1} = \frac{1}{4} N_{\text{H}} (\text{DCC})^2 \left[2J(0) + \frac{1}{2} J(\omega_{\text{H}} - \omega_{\text{C}}) + \frac{3}{2} J(\omega_{\text{C}}) + 3J(\omega_{\text{H}}) + 3J(\omega_{\text{H}} + \omega_{\text{C}}) \right] \quad (4)$$

$$\sigma = \frac{1}{4} N_{\text{H}} (\text{DCC})^2 [6J(\omega_{\text{H}} + \omega_{\text{C}}) - J(\omega_{\text{H}} - \omega_{\text{C}})] \quad (5)$$

$$\text{DCC} = -\frac{\mu_0 \gamma_{\text{C}} \gamma_{\text{H}} \hbar}{4\pi r_{\text{CH}}^3} \quad (6)$$

$$\text{NOE} = 1 + \frac{\gamma_{\text{H}}}{\gamma_{\text{C}}} \sigma T_1 \quad (7)$$

The dipole–dipole coupling constant, DCC (given in Equation (6)), depends on the CH distance r_{CH} , as well as several universal constants (permeability of vacuum, μ_0 , ^{13}C and ^1H magnetogyric ratios, $\gamma_{\text{C}}, \gamma_{\text{H}}$, and the Planck constant divided by $2\pi, \hbar$). In this work, we use the dipole coupling constant of $143.4 \times 10^3 \text{ rad s}^{-1}$, corresponding to the carbon–proton distance of 109.8 pm. N_{H} denotes the number of directly attached hydrogens – Equations (3)–(5) assume actually that the dynamics of different CH vectors is equivalent. In a more general case, and still neglecting the cross-correlations, the relaxation rates of carbons with more than one hydrogen are sums of the individual CH contributions.

The $J(\omega)$ is a reduced spectral density and its functional form depends on the model of molecular motion [16]. The formula given in Equation (8) for the spectral density $J(\omega)$ has been derived by Lipari and Szabo [17]. They considered two motions: the isotropic rotational diffusion of the molecule as a whole (with a global correlation time τ_{M}) and a much faster and restricted local motion of individual CH vectors. The two processes were assumed uncorrelated. The local motion is described by two parameters: a generalized order parameter, S^2 (defining the degree of restriction), and the local correlation time, τ_e .

$$J(\omega) = \frac{2}{5} \left[\frac{S^2 \tau_{\text{M}}}{1 + \omega^2 \tau_{\text{M}}^2} + \frac{(1 - S^2) \tau}{1 + \omega^2 \tau^2} \right] \quad (8)$$

$$\tau^{-1} = \tau_{\text{M}}^{-1} + \tau_e^{-1}$$

The situation when the molecule under investigation cannot be identified with a sphere but rather with a rigid symmetric top has been discussed by Woessner [18]. The reorientation is in this case described by two rotational diffusion constants, D_{\parallel} and D_{\perp} where D_{\parallel} accounts for rotation around the symmetry axis and D_{\perp} around the direction perpendicular to that axis. The reduced spectral density function given by Equation (9) also depends on the angle θ between the CH vector in question and the symmetry axis.

$$J(\omega) = \frac{2}{5} \sum_{k=1}^3 A_k \frac{\tau_k}{1 + \omega^2 \tau_k^2} \quad (9)$$

$$\begin{aligned} A_1 &= \frac{1}{4} (3 \cos^2 \theta - 1)^2, & \tau_1 &= \frac{1}{6D_{\perp}} \\ A_2 &= \frac{3}{4} \sin^2(2\theta), & \tau_2 &= \frac{1}{5D_{\perp} + D_{\parallel}} \\ A_3 &= \frac{3}{4} \sin^4 \theta, & \tau_3 &= \frac{1}{2D_{\perp} + 4D_{\parallel}} \end{aligned} \quad (10)$$

Relaxation parameters are also influenced by the dynamics of complex formation [19]. When the exchange rate is fast (compared to the relaxation rates) the observed longitudinal relaxation rate, $T_{1,\text{obs}}^{-1}$, and the cross-relaxation rate, σ_{obs} , are averages over free and bound forms, in analogy with the translational diffusion constants, Equation (2). The transverse relaxation is perturbed in a more subtle way since it can be enhanced by the exchange process. If the Carr–Purcell–Meiboom–Gill (CPMG) method [20, 21] is used for measuring T_2 and the exchange is fast, it was derived that [22]

$$T_{2,\text{obs}}^{-1} = (1 - p) T_{2,\text{F}}^{-1} + p T_{2,\text{B}}^{-1} + \frac{(1 - p) p \Delta \omega^2}{k_{\text{ex}}} \left[1 - \frac{\tanh(k_{\text{ex}} \tau_{1/2})}{k_{\text{ex}} \tau_{1/2}} \right] \quad (11)$$

where $\Delta \omega$ is the difference between the chemical shifts of the free and bound molecule (in angular frequency units) and $\tau_{1/2}$ is half of the echo delay used in the CPMG pulse sequence. Under advantageous conditions, the exchange rate k_{ex} can be determined when T_2 measurements are repeated for different values of $\tau_{1/2}$ (the T_2 dispersion experiment).

Experimental

Samples of 10 mM adamantanecarboxylic acid with different concentrations of β -cyclodextrin (0–25.6 mM, the solubility of β -CD is enhanced by the presence of the guest) were prepared in a solvent mixture of D_2O and $\text{DMSO}-d_6$ (7:3 molar ratio). The chemicals were purchased from Aldrich while deuterated solvents were obtained from the Cambridge Isotope Laboratories. Four samples used for relaxation measurements with the guest:host molar ratios of approximately 1:0, 1:1/2, 1:1, and 1:2 were degassed by the freeze–pump–thaw procedure (three times) and flame-sealed in 5-mm NMR tubes. The actual concentration of β -CD was

determined from the ^1H NMR spectrum in each sample using the AdCA resonances as an internal standard.

The spectra were recorded with Bruker Avance (9.4 and 11.7 T) spectrometers and with a Varian Inova spectrometer (14.1 T) at 0 and 25 °C. The temperature was calibrated prior to each experimental session, using standard methanol and ethylene glycol samples. All of the experiments were repeated at least twice. The proton and carbon resonances were assigned according to literature [6]. Typical $\pi/2$ pulse durations were 8–9 μs for ^1H and 5–7 μs or 13–16 μs for ^{13}C , depending on the probe type.

Measurements of translational diffusion coefficients were performed with the double stimulated echo experiment with bipolar pulse field gradients described by Jerschow et al. [23] This pulse sequence is optimized to suppress flow and convection artefacts (e.g., due to temperature gradient) as well as eddy current effects. The use of bipolar gradients also removes possible modulation of the intensity decay curves by chemical exchange occurring between the sites with different chemical shifts [14]. The procedure proposed by Damberg et al. [24] was used to account for gradient nonlinearity. The calibration was done on a standard sample of 1% H_2O in D_2O (doped with GdCl_3), where the value of the HDO diffusion coefficient [25] in D_2O at 25 °C was set at $1.90 \times 10^{-9} \text{ m}^2\text{s}^{-1}$. All experiments were performed using 16 different linearly spaced gradient strengths (spanning the whole range up to 60 G cm^{-1} , as declared by the manufacturer). The lengths of and delays between the gradient pulses were tuned to the best experimental conditions, depending on the temperature, and were 1–2 ms and 0.25–0.40 s, respectively. A sufficient signal-to-noise ratio in the spectra was achieved by 16 repetitions after creating a steady state by four dummy scans. The accuracy of the measurements is estimated at about 1%.

^{13}C longitudinal relaxation times T_1 were measured using the fast inversion recovery sequence [26]. The recycle delay between scans was set to at least three times the longest T_1 and 10–15 different relaxation delays were used. The number of scans was typically about 1000. Proton decoupling according to the WALTZ16 pulse scheme [27] was turned on during the whole execution of the sequence at a power level corresponding to the proton $\pi/2$ pulse duration of ca. 100 μs . The T_1 values were obtained by three-parameter exponential fitting of the signal intensities.

For measuring $^{13}\text{C}\{-^1\text{H}\}$ steady-state NOE enhancements we used the dynamic NOE sequence [28] with one very short (0.1 ms) and one long (about five times the longest T_1) proton irradiation period (WALTZ16 as above). The NOE value was determined as the ratio of the corresponding signal intensities in the two spectra. The recycle delay was set to 8–10 times the T_1 to allow for complete relaxation between scans and the number of acquisitions was about 2000.

To increase the sensitivity, the ^{13}C transverse relaxation times, T_2 , were measured using inverse detection with a two-dimensional heteronuclear correlation method [29, 30]. In order to avoid excitation of the three-spin order terms in the CH_2 spin systems, prior to the CPMG relaxation segment, the first INEPT magnetization transfer was removed. The CPMG single echo duration was 900 μs and it was varied from 400 to 2000 μs in the T_2 dispersion experiment. Ten to 14 relaxation delays were used together with two-parameter exponential fit of signal intensities to calculate T_2 values. The accuracy of the T_1 and T_2 values is estimated to be better than 5%, while the uncertainty of the NOE values is about 10%.

The NOESY spectrum [31] with a residual water signal suppressed by excitation sculpting method [32] was recorded at 9.4 T and 25 °C using a mixing time of 300 ms.

Results

Description of NMR spectra

^1H and ^{13}C spectra of the AdCA: β -CD complex are shown in Figure 2 (see also Figure 1 for atom numbering). The chemical shifts of proton as well as carbon resonances change only very slightly (by less than 0.1 ppm for protons and about 0.2 ppm for carbons) among the samples with different host concentrations. The most remarkable difference was observed on the resonances of the two δ -protons of AdCA – they are not magnetically equivalent and, when the molecule is free in solution, they give rise to a strongly coupled doublet of doublets. For AdCA incorporated in the complex, the two resonances overlap and only a single broad line is observed. Minor changes of the β -CD proton peaks were difficult to follow, due to their mutual overlap. The ^{13}C spectrum of β -CD contains six lines, corresponding to the six carbons in a glucose unit. For the AdCA, only the γ and δ sites are well resolved in the carbon frequency dimension, the other aliphatic carbons being hidden within the strong DMSO- d_6 multiplet. The carbonyl resonance was left outside of the spectral range.

The NOESY spectrum of the sample with excess of the host (25 °C) was recorded in order to explore the spatial proximity of the different sites in the AdCA and β -CD molecules. Relatively strong cross-peaks between β , γ and δ proton resonances of the guest and the group of overlapping peaks corresponding to protons 3, 5 and 6 of β -CD were observed. For the mixing time of 300 ms that was used in our case, we also observe much weaker cross-peaks to all other β -CD protons.

Complexation process

For characterization of the complexation process between AdCA and β -CD, we choose to follow changes in the diffusion coefficient of the AdCA molecule during

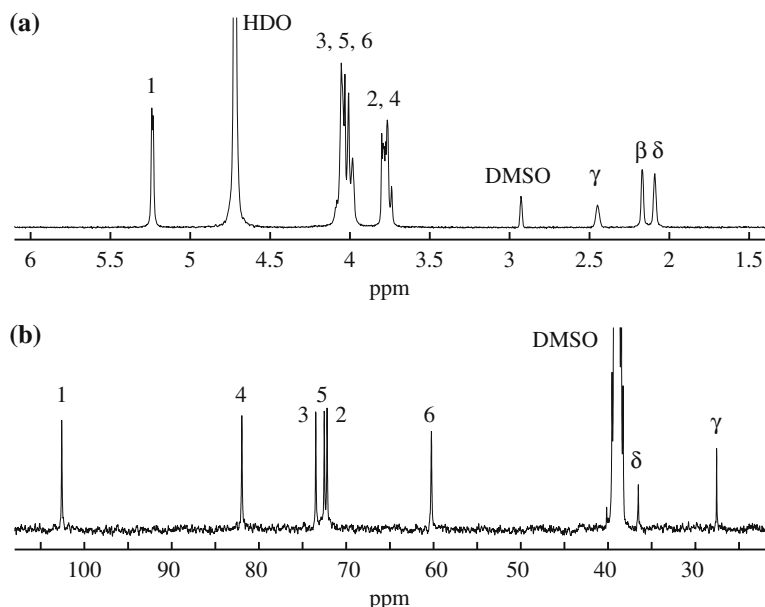


Figure 2. ^1H (a) and ^{13}C (b) NMR spectra of the AdCA: β -CD complex at 9.4 T and 25 $^\circ\text{C}$ in $\text{D}_2\text{O}/\text{DMSO}-d_6$ solvent (the concentrations of the guest and the host are 10 and 17.3 mM, respectively).

titration with β -CD. The overlap of the β -CD proton resonances does not prevent this analysis since all the lines decay with the same constant. The diffusion coefficients were determined for each peak (or group of peaks) and the results were averaged to get a single value per molecule. All the samples contained 10 mM AdCA and β -CD concentration was varied from 0 to 25.6 mM. With the increasing amount of β -CD, we observed changes in the viscosity of the solution which was reflected in a reduced water diffusion constant. The measured diffusion coefficients were therefore viscosity-corrected prior to further analysis, making use of the solvent properties as an internal standard.

The changes in the observed diffusion coefficient of AdCA were fitted by optimizing the diffusion coefficient

of the complex, D_B , and the dissociation constant, K_d . The diffusion coefficient for free AdCA, D_F , was measured directly and was kept fixed. The results are presented in Figure 3 for both temperatures. The error limits were estimated by Monte Carlo simulations. At 25 $^\circ\text{C}$, the 1:1 stoichiometry model gives an excellent fit, with the dissociation constant $K_d = 0.71 \pm 0.07$ mM. At 0 $^\circ\text{C}$, however, this model deviates from the experimental data (full line in Figure 3 panel B, $K_d = 0.09$ mM). The apparent diffusion coefficient decreases faster than the 1:1 model is able to explain. It suggests that including the 2:1 stoichiometry, where two AdCA molecules are attached to one β -CD molecule, will describe the experimental data better. Indeed, the dashed curve representing this model improves the fit significantly (see Figure 3,

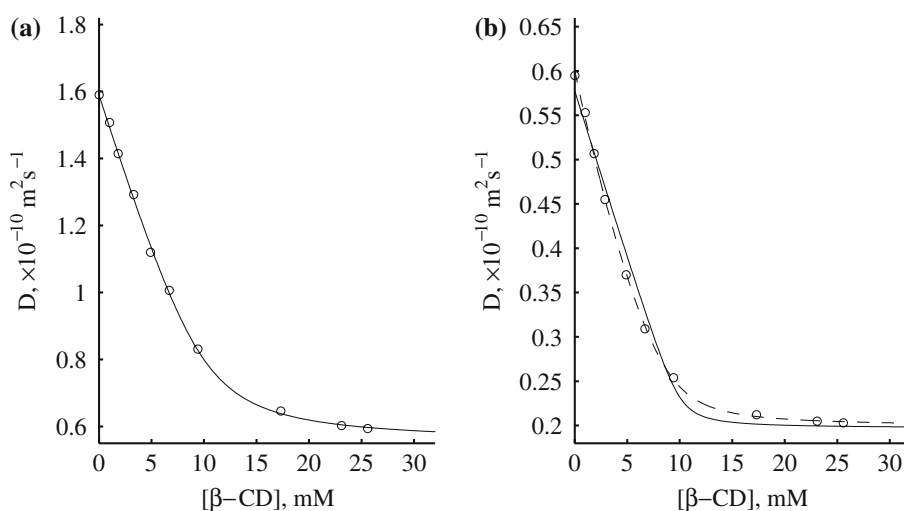


Figure 3. Diffusion coefficient of AdCA at 25 $^\circ\text{C}$ (a) and 0 $^\circ\text{C}$ (b) as a function of the β -CD concentration. The solid curves correspond to the fit assuming the 1:1 (guest:host) stoichiometry of the complex whereas the dashed curve represents the 2:1 binding model.

panel B) and yields the two dissociation constants, $K_{d1} = 0.26 \pm 0.04$ mM and $K_{d2} = 16.4 \pm 1.4$ mM, for stepwise formation of the 1:1 and 2:1 complexes, respectively. The reverse complexation model, where one molecule of AdCA is trapped between the two β -CD molecules (1:2 stoichiometry), does not improve the fit compared to the 1:1 model only. Furthermore, no corresponding changes in the β -CD diffusion coefficient were observed.

¹³C relaxation

The relaxation parameters for the five ring carbons (C-1–C-5) were in all cases very similar. In agreement with the earlier work of Kowalewski and Widmalm [33], who measured ¹³C relaxation of α - and γ -cyclodextrins, we adopt the concept of dynamic equivalence of these carbons and report only averaged values. No changes of T_1 , NOE and T_2 for the β -CD carbons were observed for samples with different guest:host concentration ratios and we conclude that the presence of the guest has no effect on the relaxation of the host. This is perhaps not surprising, when we compare molecular weights of β -CD and AdCA (the guest is approximately six times lighter than the host). The overall shape of the complex is also very similar to β -CD alone, suggesting that the overall reorientational dynamics of the host should not be affected by the complex formation. The T_2 values, however, require a more careful consideration since they can possibly be reduced by the chemical exchange process. The exchange contribution to the transverse relaxation rate, given by the last term of Equation (11), is scaled by the product of the populations of free and complexed forms. This factor changes dramatically between the samples with 4.9 mM and 17.3 mM β -CD concentration, but still the same T_2 values were measured in both cases. From this observation, we conclude that the chemical exchange has no effect on the trans-

verse relaxation of β -CD carbons, probably due to the combination of small differences in chemical shifts and a fast exchange rate. All experimental data for β -CD carbons are summarized in Tables 1 and 2. For the exocyclic hydroxymethyl carbons, the NOE is increased only slightly, compared to the CH carbons, the T_1 values are reduced almost by half, which is related to the factor N_H in Equation (3), while the T_2 data change less.

Measurements performed on the sample of pure AdCA yielded relaxation data for the free guest directly. For the bound form of AdCA, experiments on the samples with 4.9, 9.4 and 17.3 mM concentration of β -CD were analyzed at 25 °C. The observed values of the longitudinal relaxation rate, $T_{1,obs}^{-1}$, and the cross-relaxation rate, σ_{obs} , are population-weighted averages of free and bound forms. Since the dissociation constant was determined previously by diffusion measurements, the mole fraction of the complexed AdCA, p , was calculated from Equation (1). Equations (12) and (13) were then used to extract the relaxation time, $T_{1,B}$, and the cross-relaxation rate, σ_B , by least-square fitting of experimental data (indices F and B correspond to free and bound state of AdCA, respectively).

$$\frac{1}{T_{1,obs}} = \frac{1-p}{T_{1,F}} + \frac{p}{T_{1,B}} \quad (12)$$

$$\text{NOE}_{obs} = 1 + [(1-p)\sigma_F + p\sigma_B]T_{1,obs} \quad (13)$$

A representative example of this analysis is given in Figure 4. In principle, experiments at only one β -CD concentration are sufficient to determine $T_{1,B}$ and σ_B . Making use of several measurements, however, reduces experimental uncertainties.

On the sample with 1:1/2 AdCA: β -CD concentration ratio, the T_2 measurements with different echo delays $\tau_{1/2}$ were performed in order to investigate the exchange process. This sample was selected for a more careful exchange study since the product $(1-p)p$

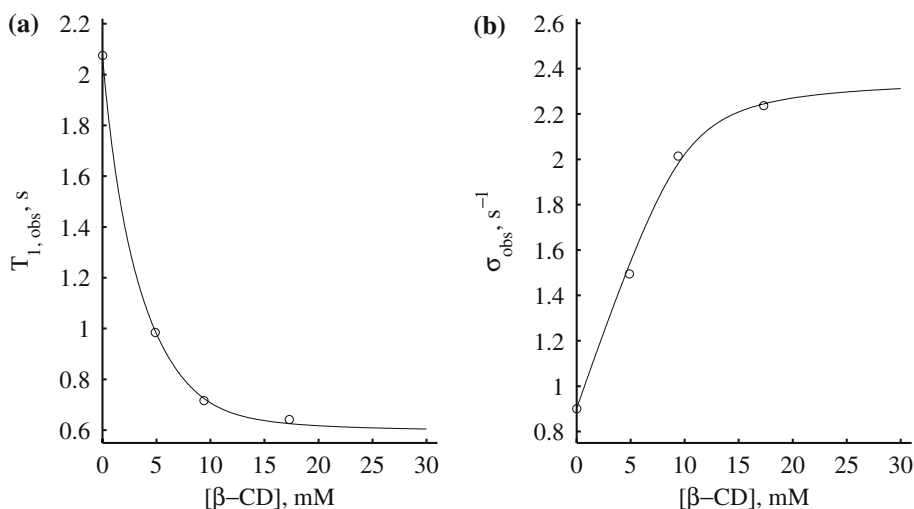


Figure 4. Representative examples of the extraction of relaxation data for AdCA molecule bound in a complex with β -CD at 25 °C. The experiments were performed on samples with different β -CD concentrations and the observed values of longitudinal relaxation time ($T_{1,obs}$, panel a) and cross-relaxation rate (σ_{obs} , panel b) were fitted according to the 1:1 (guest:host) binding model.

(compare Equation (11)) is largest in this case. No significant changes of the observed T_2 were detected over the range of $\tau_{1/2}$ from 200 μs to 1000 μs . From the inspection of Equation (11), we see that the exchange contribution (last term on the right-hand side) does not depend on $\tau_{1/2}$ when $\tau_{1/2} \gg k_{\text{ex}}^{-1}$. This condition, however, does not imply that chemical exchange has no effect at all – the transverse relaxation rate can still be enhanced by an amount $(1-p)p\Delta\omega^2k_{\text{ex}}$. Nevertheless, analyzing apparent T_2 values for samples of different guest:host concentration ratios (and thus different values of p), it was found that the exchange contribution does not exceed limits given by experimental errors. Therefore, the same procedure as for T_1 was applied to get transverse relaxation times of the bound AdCA at 25 °C.

The procedure described above is not applicable to the data obtained at 0 °C because of possible 2:1 complexes, in which AdCA can have different properties. On the other hand, the composition of the sample with 10 mM AdCA and 17.3 mM β -CD is such that 93% of the AdCA molecules are bound in 1:1 complex (3% is the population of free AdCA and 4% is bound in the 2:1 complex). The data acquired for this sample mainly reflect the relaxation properties of the guest associated with β -CD in the 1:1 stoichiometry, and are used as such without any further corrections. A possible influence of chemical exchange on the transverse relaxation of the guest was excluded using the same experimental evidence and arguments as at 25 °C. The relaxation parameters for the free and bound AdCA are collected in Tables 1 and 2, corresponding to 25 °C and 0 °C, respectively.

Discussion

Complex

The complexation of AdCA with β -CD was studied by several groups during the past [4]. Cromwell and co-workers [5] reported a strong binding of AdCA in the 1:1 stoichiometry at a guest concentrations about 1 mM in water. Breslow et al. [34], on the other hand, have observed evidence for the 2:1 AdCA: β -CD complex formation at higher concentrations. Also a molecular-modelling study of bromoadamantane: β -CD complexes, published by Ivanov and Jaime [35], describes the association of a second guest molecule as an energetically favorable process. The structure proposed in the latter work contains one bromoadamantane fully incorporated inside the β -CD cavity, whereas the second guest molecule is located at the primary rim of β -CD. This agrees well with experiments, performed by Breslow et al. [34] on β -CD modified at primary hydroxyl groups, where no evidence for the 2:1 complexation was observed – the modification prevented the binding of the second guest.

In our study, we work with 10 mM concentration of AdCA in the $\text{D}_2\text{O}/\text{-DMSO}$ solvent mixture. The stability of the complexes may be altered compared to the case of water as solvent, since hydrophobic interactions contribute significantly to the association process [36], even if the van der Waals forces are believed to be the major contributor. The diffusion experiments at 25 °C suggest that binding of the second AdCA is negligible and the data are fully consistent with the 1:1

Table 1. Relaxation parameters for β -cyclodextrin and adamantanecarboxylic acid, free in solution and bound in the complex, obtained at several magnetic fields and 25 °C

		9.4 T		11.7 T			14.1 T	
		T_1 (s)	NOE	T_1 (s)	NOE	T_2 (s)	T_1 (s)	NOE
β -CD	C-1-C-5	0.23	1.25	0.35	1.23	0.078	0.42	1.18
	C6	0.12	1.30	0.19	1.26	0.061	0.22	1.20
Free	C_γ	2.09	2.95	2.08	2.87	1.98	2.54	3.00
AdCA	C_δ	0.45	2.95	0.43	2.57	0.45	0.52	2.90
Bound	C_γ	0.59	2.50	0.59	2.40	0.42	0.69	2.13
AdCA	C_δ	0.20	1.70	0.25	1.80	0.061	0.29	1.80

Table 2. Relaxation parameters for β -cyclodextrin and adamantanecarboxylic acid, free in solution and bound in the complex, obtained at several magnetic fields and 0 °C

		9.4 T		11.7 T			14.1 T	
		T_1 (s)	NOE	T_2 (s)	T_1 (s)	NOE	T_1 (s)	NOE
β -CD	C-1-C-5	0.50	1.24	0.034	0.73	1.20	1.01	1.22
	C-6	0.24	1.27	0.027	0.38	1.20	0.51	1.23
Free	C_γ	1.30	2.53	1.15	1.33	2.33	1.39	2.4
AdCA	C_δ	0.27	2.30	0.27	0.26	2.10	0.30	1.9
Bound	C_γ	0.39	2.12	0.18	0.43	2.11	0.53	1.95
AdCA	C_δ	0.23	1.93	0.061	0.26	1.80	0.36	1.95

stoichiometry. At the lower temperature, however, the presence of the 2:1 complex becomes detectable.

Cromwell et al. [5] also showed that the dissociation constant for the protonated form of AdCA is 15–20 times smaller than for the anionic form. The proton dissociation was not considered in our analysis and the pH in the sample solutions was not fixed. Thus, the dissociation constant K_d for the AdCA: β -CD complex only represents an apparent value, which is hard to compare with literature. We want to stress that the determination of the equilibrium constant only provides the molar ratios and is used to determine the relaxation properties of the bound guest. Since AdCA is a weak acid [5] ($\text{p}K_a=4.9$), it exists in the aqueous solution predominantly in the neutral form. By addition of β -CD, the neutral form is further stabilized by the inclusion into the cavity. It seems therefore safe to assume that the relaxation parameters reflect the properties of the acid and not of its anion.

To confirm the deep penetration of AdCA into the β -CD cavity, a NOESY spectrum was acquired. It agrees nicely with previous studies in aqueous solutions [37]. A quantitative analysis of the cross-peak intensities is complicated by the exchange process. While in Figure 1 we provide only a simplified drawing, a probable solution structure of a complex with similar guest can be found in the study by Ivanov and Jaime [35]. The X-ray structure was solved by Hamilton [38].

NMR relaxation of the host

As indicated in the result section, the presence of AdCA in the cavity can be disregarded in discussion of ^{13}C relaxation of the host. The NMR relaxation of α - and γ -cyclodextrins was studied in detail in the previous work from our laboratory [33]. In the interpretation of the relaxation data for β -CD, we follow a similar procedure. The five ring carbons in each glucose unit of β -CD are treated as dynamically equivalent and the averaged values are used. The two sets of relaxation parameters, for the methine and hydroxymethylene carbons, are treated separately and are both fitted according to the Lipari–Szabo model, Equation (8), optimizing simultaneously τ_M , S^2 and τ_e with a restriction to non-negative values. The results are presented in Table 3. When the order parameter attains values close to 1, which is the case for the methine carbons, the fit is insensitive to the local correlation time, τ_e . Repeated

Table 3. Motional parameters obtained from the Lipari–Szabo analysis of the relaxation data of β -cyclodextrin at two temperatures^a

Temperature	Group	τ_M (ns)	S^2	τ_e (ps)
25 °C	CH	2.94 ± 0.14	0.91 ± 0.03	60 ± 130
	CH ₂	2.19 ± 0.11	0.72 ± 0.02	11 ± 9
0 °C	CH	7.60 ± 0.30	0.91 ± 0.03	40 ± 70
	CH ₂	5.80 ± 0.20	0.73 ± 0.02	9 ± 6

^a The standard deviations were obtained from a Monte Carlo simulation.

calculations for the methines, with τ_e fixed at several values, produced results within error limits determined by Monte Carlo simulations (assuming standard deviations of 5% for the relaxation rates and of 10% for the NOE).

In general, our present results on β -CD reflect all features found for α - and γ -cyclodextrins [33]. The global correlation time, τ_M , for hydroxymethyl groups predicted from a separate fit is about 25% shorter than for the ring carbons at both temperatures. The two groups were also treated jointly, with one common global correlation time (not shown). However, this produced a poorer fit and resulted in a value of τ_M in-between the two reported in Table 3. The local motion parameters do not depend significantly on the procedure chosen, and are basically equal for different fits considering their error limits. The glucose ring is found fairly rigid whereas the hydroxymethyl groups show more extensive local motion. The same order parameters were found at 0 °C and 25 °C. The global correlation times are longer at lower temperature, as expected, and the change corresponds to an Arrhenius activation energy of approximately 26 kJ mol^{-1} , virtually the same as for the other two cyclodextrins.

The explanation for shorter τ_M values for the hydroxymethyl carbons, obtained in the separate Lipari–Szabo fits, can be sought in more complicated local motions of these groups. In the recent study by Köver et al. [39], the internal dynamics of the CH₂OH group in methyl- β -D-glucopyranoside is described using three types of motion. The first two are the same as in the Lipari–Szabo approximation. In addition, an evidence is found for a third motion, on a time scale intermediate between the global and the local correlation times, modelled as two-site jumps between different conformations of the hydroxymethyl group. When this additional motion is ignored, the result may be a shortening of τ_M , observed for cyclodextrins.

NMR relaxation of the guest

The shape of the AdCA molecule resembles a symmetric top. It is therefore plausible to interpret the relaxation data of the free guest using the rotational diffusion constants D_{\parallel} and D_{\perp} , defining the spectral density given in Equation (9). The main axis is identified with the C_3 symmetry axis of the adamantyl moiety. A rigid structure, with a tetrahedral geometry, is assumed for all carbons when determining the angles θ between the CH vectors and the main axis. It is worth to note that one of the CH vectors for the δ -carbon is parallel to the symmetry axis, and is referred to as the “parallel vector” further in the text. These definitions are illustrated in Figure 1.

The results representing the best fit of the rotational diffusion constants, D_{\parallel} and D_{\perp} , to the experimental data at 25 °C are presented in Table 4. The rotation around the main axis is very fast, with the characteristic time $\tau_e = 1/(6D_{\parallel})$ being 5.6 ps. This motion can be

Table 4. Rotational diffusion constants of AdCA free in solution determined at two temperatures^a

	D_{\parallel}	D_{\perp}	D_{\parallel}/D_{\perp}
25 °C	2.97 ± 0.28	0.185 ± 0.009	16.1
0 °C ^b	1.75 ± 0.21	0.102 ± 0.008	17.2

^a The values are in units of 10^{10} s^{-1} , the standard deviations were obtained from a Monte Carlo simulation.

^b The fit is based on experimental T_1 and T_2 values only.

considered as a relatively free rotation around the C—COOH bond, even if the acid group is “fixed” by interactions with a solvent. It is probably this effect that is responsible for the hindered rotation around the perpendicular axis. The anisotropy of the molecular motion is reflected in the ratio D_{\parallel}/D_{\perp} . High values of this parameter were found in other solvents as well [40], with AdCA showing a striking anisotropic behavior, compared to other adamantane derivatives. When assessing the time scale of the perpendicular rotation, we can note that the molecular motion is departing slightly from the limit of extreme narrowing. This feature is manifested in the values of the NOE factors somewhat reduced with respect to the limit value of 2.99 (see Table 1), especially clear for the δ -carbon which is most sensitive to the slower rotational mode.

The analysis of the 0 °C data for free AdCA is more complicated. We were not able to obtain satisfactory fits of the T_1, T_2 and NOE data in Table 2 to the symmetric top model. Excluding the NOEs, the fit resulted in the data in Table 4; the rotational diffusion coefficients are about 60% smaller than those at 25 °C. A tentative explanation of the difficulties may perhaps be sought in self-association of AdCA. The presence of a small amount of a larger species with a slower rotational motion, in fast exchange with the monomer, might explain the experimental observations.

We turn now to the analysis of the data for the bound guest. In our previous studies of reorientational behavior of host–guest complexes [10, 11], we treated the motion of the bound guest in terms of the Lipari–Szabo approach. The global reorientation is controlled by the big host molecule, while the guest dynamics is considered as a local motion. We begin the discussion with the analysis of the bound AdCA relaxation data acquired at 25 °C, using the spectral density described in Equation (8). The global correlation time, τ_M , and a pair

of S^2, τ_e values for each carbon were optimized simultaneously to reproduce the experimental values. The results are given in Table 5, fit A. All the following fits are also graphically presented in Figure 5. The Monte Carlo error analysis of the 25 °C data was based on the assumed standard deviations of 5% for the relaxation rates and of 10% for the NOE. The fit yielded a τ_M value of 3.3 ns, which is very close to 2.9 ns, obtained for β -CD ring carbons. When the τ_M value is fixed at 2.9 ns, the fit of AdCA data gives almost identical local parameters. The order parameter for the γ -carbon is very low, whereas the δ -carbon shows an intermediate value. It is reasonable to assume that the reorientation of AdCA inside the β -CD cavity is highly anisotropic and that the two CH vectors of the δ -carbon experience different motions. Thus, one might associate the order parameters and the local correlation times with the CH vectors rather than with carbon atoms. In the next fit, we divide the CH vectors into two categories. The parallel vector is considered for itself, while the other CH vector of the δ -carbon is assumed dynamically equivalent with the CH vector of the γ -carbon. The two types of vectors are characterized by distinct sets of parameters. The results are given in Table 5, fit B. We can see that while the local parameters of the γ -carbon remain the same, the order parameter of the parallel CH vector now attains a very high value. This corresponds to a strong restriction of the motional freedom of the latter vector. In fact, the order parameter for the δ -carbon from the fit A can be thought of as an average of the two values from the fit B. This situation can be understood in terms of the rotation of AdCA around its C_3 axis, which may coincide with the symmetry axis of the cyclodextrin, being the most important local motion. This, in turn, brings us an idea that the motion of the bound AdCA can perhaps still be viewed as a symmetric top reorientation. The third fit (referred as C in Table 5), according to Equations (9) and (10), is not as good as the previous two, in the sense that it does not reproduce the δ -carbon data with the same accuracy. Nevertheless, it reflects nicely the time scales of the motions involved. The rotation of AdCA inside the cavity occurs with a correlation time $\tau_c = 1/(6D_{\parallel}) = 24 \text{ ps}$, while the rotation around the perpendicular direction is characterized by $\tau_c = 1/(6D_{\perp}) = 3.3 \text{ ns}$, again very close to τ_M of β -CD. Obviously, the AdCA reorientation around the

Table 5. Motional parameters of AdCA bound inside the β -CD cavity, determined at 25 °C by fitting various models^a

Fit A	$\tau_M = 3.28 \pm 0.18 \text{ ns}$		
	γ -carbon	$S^2 = 0.08 \pm 0.01$	$\tau_e = 75 \pm 5 \text{ ps}$
	δ -carbon	$S^2 = 0.46 \pm 0.02$	$\tau_e = 64 \pm 6 \text{ ps}$
Fit B	$\tau_M = 3.28 \pm 0.19 \text{ ns}$		
	CH non-parallel	$S^2 = 0.09 \pm 0.02$	$\tau_e = 74 \pm 5 \text{ ps}$
	CH parallel	$S^2 = 0.83 \pm 0.04$	$\tau_e = 25 \pm 25 \text{ ps}$
Fit C	$D_{\parallel} = (68.6 \pm 4.2) \times 10^8 \text{ s}^{-1}$	$D_{\perp} = (0.50 \pm 0.03) \times 10^8 \text{ s}^{-1}$	

^a Fits A and B correspond to the Lipari–Szabo model with local parameters (S^2, τ_e) associated with carbon atoms and CH vectors, respectively. Fit C is the symmetric top model. The standard deviations were obtained from a Monte Carlo simulation.

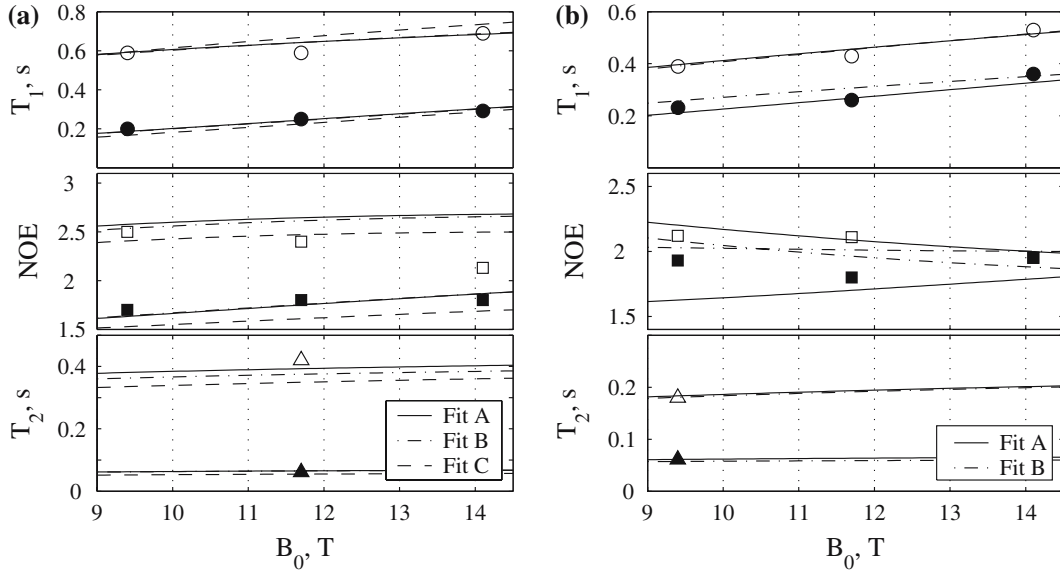


Figure 5. Graphical presentation of the fits to the relaxation parameters for AdCA bound in the complex, obtained at 25 °C (a) and 0 °C (b). Open symbols correspond to γ -carbon while full symbols to δ -carbon. The parameters of individual fits are summarized in Tables 5 and 6.

perpendicular axis has to occur together with the surrounding host molecule.

Fitting the Lipari–Szabo spectral density to the relaxation data of AdCA obtained at 0 °C did not give any satisfactory results. When all motional parameters were optimized, the global correlation time, τ_M , reached the value of 3.6 ns, very far from the 7.6 ns for β -CD. The fit with a τ_M fixed at 7.6 ns showed large discrepancies with the experiments. At 25 °C, we described the reorientation of the guest inside the host’s cavity as a rotation around the cyclodextrin symmetry axis, coinciding with the C_3 axis of the adamantyl moiety. The AdCA molecule can, however, also tilt to one side or another, with the acid group approaching different glucose units of the cyclodextrin. These two motions – rotation and “rocking” – can, in principle, occur on separate time scales. Then, the spectral density proposed by Clore et al. [41] may be a more appropriate model. The two motions are characterized by local correlation times, τ_f, τ_s , and generalized order parameters, S_f^2, S_s^2 , for the faster and the slower motion, respectively. Assuming isotropic overall reorientation, the spectral density takes the form

$$J(\omega) = \frac{2}{5} \left[\frac{S^2 \tau_M}{1 + \omega^2 \tau_M^2} + \frac{(1 - S_f^2) \tau_f}{1 + \omega^2 \tau_f^2} + \frac{(S_f^2 - S^2) \tau_s}{1 + \omega^2 \tau_s^2} \right] \quad (14)$$

$$\tau_F^{-1} = \tau_M^{-1} + \tau_f^{-1} \quad \tau_S^{-1} = \tau_M^{-1} + \tau_s^{-1}$$

where the total generalized order parameter S^2 comprises dependency on both S_f^2 and S_s^2 .

Indeed, the fit according to Equation (14), with local parameters ($S^2, S_f^2, \tau_s, \tau_f$) associated with each carbon, improved the agreement between the calculated and experimental data to a satisfactory level. In order to reduce the number of variables, the global correlation time was kept fixed at 7.6 ns (the value for β -CD) and the results are given in Table 6, fit A (see also comparison in Figure 5b). The error analysis using Monte Carlo simulations shows that local correlation times are quite poorly determined. It should be noted that somewhat larger standard deviations of 7% and 15% were assumed in this case, to account for the uncertainty in the solution composition. The situation is worst for τ_s of the δ -carbon, which attains perhaps unrealistically high value. However, the fit is rather insensitive to this parameter which can be understood from the inspection of Equation (14) and the observation that S^2 and S_f^2 are quite close to each other.

One can consider analyzing the dynamics in terms of the parallel and non-parallel CH-vectors, rather than carbon atoms, also at this temperature. We have applied a slightly different strategy to each of the two types of

Table 6. Motional parameters of AdCA bound inside the β -CD cavity, determined at 0 °C by fitting various models^a

Fit	Carbon Type	S^2	S_f^2	τ_s	τ_f
Fit A	γ -carbon	0.09 ± 0.01	0.49 ± 0.11	0.43 ± 0.22 ns	40 ± 30 ps
	δ -carbon	0.15 ± 0.06	0.41 ± 0.07	2.3 ± 2.2 ns	44 ± 22 ps
Fit B	CH non-parallel	0.09 ± 0.01	0.49 ± 0.10	0.50 ± 0.24 ns	34 ± 25 ps
	CH parallel	0.35 ± 0.05	$\tau_e = 43 \pm 19$ ps		

^a Fit A uses spectral density in the form of Equation (14) with local parameters ($S^2, S_f^2, \tau_s, \tau_f$) associated with carbons. In model B, non-parallel CH vectors are described using Equation (14) while the parallel vector using Equation (8). In both cases, the global correlation time was kept fixed at the value obtained for ring carbons of β -CD, $\tau_M = 7.6$ ns. The standard deviations were obtained from a Monte Carlo simulation.

vectors. The non-parallel vectors can be subject to both motions (rocking, rotation) mentioned above and should thus be treated according to Equation (14). On the other hand, the rotation does not affect the parallel CH vector of the δ -carbon and its dynamics can be described by the Lipari–Szabo spectral density. The analysis along these lines provided a reasonable agreement with the experiments and the results are given in Table 6, fit B. It is tempting to use this finding to speculate about which motion is responsible for the slower and faster component in the spectral density. We note that the local correlation time of the parallel vector turns out to be of similar magnitude as τ_f for the other vectors. This observation indicates that the fast motion is the one which has a similar effect on both CH vectors, which excludes the rotation. Thus, perhaps surprisingly, the rotation is assigned as the slower motion. We want to emphasize that the conclusion of this tentative analysis should be treated just as a hypothesis.

The data acquired at 25 °C do not indicate the presence of local motions on different time scales. A plausible explanation of this difference between the two temperatures may be that at room temperature both local motions are in extreme narrowing and, thus, the separation of the two reorientational modes is not possible.

Conclusion

The formation of an inclusion complex between adamantanecarboxylic acid and β -cyclodextrin was studied in the D₂O/DMSO solvent mixture by means of translational diffusion measurements. The pulsed field gradient methods provide accurate diffusion coefficients, especially when corrections for the gradient non-linearities are taken into account. The changes in apparent diffusion properties of AdCA during the titration by β -CD are fully described by formation of 1:1 complex at 25 °C. However, at 0 °C the data indicate the presence of a 2:1 (guest:host) complex. Similar findings were reported earlier in the literature.

Determination of the dissociation constant allowed us to extract ¹³C NMR relaxation parameters of the AdCA molecule bound in the β -CD cavity. The reorientation of the free guest could at room temperature be modelled as a rotation of a symmetric top and was found to be very anisotropic. This anisotropy can be ascribed to interactions of the acid group with surrounding solvent molecules. When AdCA is bound inside the cavity, its reorientation at room temperature can be described by either the Lipari–Szabo approach or the axially symmetric rotational diffusion model, in the latter case with extremely high anisotropy. Despite the high association constant ($K_a = 1/K_d = 1400 \text{ M}^{-1}$), which suggests a strong interaction between the two molecules, AdCA rotates fast around the β -CD symmetry axis. This motion is made possible by the spherical shape of the adamantyl moiety and the whole system resembles of a “molecular bear-

ing”. Lowering the temperature leads to a separation of local motional modes to different time scales. The relaxation properties are no longer possible to explain using the two-step Lipari–Szabo or the symmetric top models. Instead, the data were analyzed using the extended, three-step spectral density proposed by Clore et al. [41].

Acknowledgements

This work has been supported through a grant from the Swedish Research Council. This work is also a part of the research plan MS 0021620835 that is financed by the Ministry of Education of the Czech Republic.

References

1. D.M. Rudkevich: *Bull. Chem. Soc. Jpn* **75**, 393 (2002).
2. J. Szejtli: *Chem. Rev.* **98**, 1743 (1998).
3. L. Liu and Q.-X. Guo: *J. Incl. Phenom.* **42**, 1 (2002).
4. M.V. Rekharsky and Y. Inoue: *Chem. Rev.* **98**, 1875 (1998).
5. W.C. Cromwell, K. Byström, and M.R. Eftink: *J. Phys. Chem.* **89**, 326 (1985).
6. H.-J. Schneider, F. Hacket, V. Rüdiger, and H. Ikeda: *Chem. Rev.* **98**, 1755 (1998).
7. M. Pons and O. Millet: *Progr. NMR Spectr* **38**, 267 (2001).
8. G.S. Kottas, L.I. Clarke, D. Horinek, and J. Michl: *Chem. Rev.* **105**, 1281 (2005).
9. J.P. Behr and J.M. Lehn: *J. Am. Chem. Soc.* **98**, 1743 (1976).
10. J. Lang, J.J. Dechter, M. Effemey, and J. Kowalewski: *J. Am. Chem. Soc.* **123**, 7852 (2001).
11. Z. Tošner, J. Lang, D. Sandström, O. Petrov, and J. Kowalewski: *J. Phys. Chem. A* **106**, 8870 (2002).
12. L. Fielding: *Tetrahedron* **56**, 6151 (2000).
13. R. Wimmer, F.L. Aachmann, K.L. Larsen, and S.B. Petersen: *Carbohydr. Res.* **337**, 841 (2002).
14. C.S. Johnson: *Progr. NMR Spectr.* **34**, 203 (1999).
15. D. Canet: *Nuclear Magnetic Resonance – Concepts and Methods*, John Wiley, Chichester (1996).
16. P. Luginbühl and K. Wüthrich: *Progr. NMR Spectr.* **40**, 199 (2002).
17. G. Lipari and A. Szabo: *J. Am. Chem. Soc.* **104**, 4546 (1982).
18. D.E. Woessner: *J. Chem. Phys.* **37**, 647 (1962).
19. D.E. Woessner: in D.M. Grant and R.K. Harris (eds.), *Encyclopedia of Nuclear Magnetic Resonance*, Vol. 6, Chichester, UK (1996), pp. 4018–4028.
20. H.Y. Carr and E.M. Purcell: *Phys. Rev.* **94**, 630 (1954).
21. D. Meiboom and S. Gill: *Rev. Sci. Instrum.* **29**, 688 (1958).
22. Z. Luz and S. Meiboom: *J. Chem. Phys.* **39**, 366 (1963).
23. A. Jerschow and N. Müller: *J. Magn. Reson.* **125**, 327 (1997).
24. P. Damberg, J. Jarvet, and A. Gräslund: *J. Magn. Reson.* **148**, 343 (2001).
25. L.G. Longworth: *J. Phys. Chem.* **64**, 1914 (1960).
26. D. Canet, G.C. Levy, and I.R. Peat: *J. Magn. Reson.* **18**, 199 (1975).
27. A.J. Shaka, J. Keeler, and R. Freeman: *J. Magn. Reson.* **53**, 313 (1983).
28. J. Kowalewski, A. Ericsson, and R. Vestin: *J. Magn. Reson.* **31**, 165 (1978).
29. L.E. Kay, L.K. Nicholson, F. Delaglio, A. Bax, and D.A. Torchia: *J. Magn. Reson.* **97**, 359 (1992).
30. A.G. Palmer, N.J. Skelton, W.J. Chazin, P.E. Wright, and M. Rance: *Mol. Phys.* **75**, 699 (1992).
31. J. Jeener, B.H. Meier, P. Bachman, and R.R. Ernst: *J. Chem. Phys.* **71**, 4546 (1979).
32. T.-L. Hwang and A.J. Shaka: *J. Magn. Reson. A* **112**, 275 (1995).
33. R. Kowalewski and G. Widmalm: *J. Phys. Chem.* **98**, 28 (1994).
34. R. Breslow, M.F. Czarniecki, J. Emert, and H. Hamagichi: *J. Am. Chem. Soc.* **102**, 762 (1980).

35. P.M. Ivanov and C. Jaime: *J. Mol. Struct.* **377**, 137 (1996).
36. J.C. Harrison and M.R. Eftink: *Biopolymers* **21**, 1153 (1982).
37. V. Rüdiger, A. Eliseev, S. Simova, H.-J. Schneider, M.J. Blandamer, P.M. Cullis, and A.J. Meyer: *J. Chem. Soc., Perkin Trans 2*, 2119 (1996).
38. J.A. Hamilton and M.N. Sabesan: *Acta Cryst. B* **38**, 3063 (1982).
39. K.E. Kövér, G. Batta, J. Kowalewski, L. Ghalebani, and D. Kruk: *J. Magn. Reson.* **167**, 273 (2004).
40. H. Beierbeck, R. Martino, and J.K. Saunders: *Can. J. Chem.* **57**, 1224 (1979).
41. G.M. Clore, A. Szabo, A. Bax, L.E. Kay, P.C. Driscoll, and A.M. Gronenborn: *J. Am. Chem. Soc.* **112**, 4989 (1990).